IRSTI 29.27.51 https://doi.org/10.26577/phst2024v11i2b09

Effects of increasing applied voltage and frequency on plasma parameters in dielectric barrier discharge plasma

Ibrahim K. Abbas

Department of Physics, College of Science, University of Baghdad, Baghdad, Iraq
e-mail: Ibrahim.kareem1104a@sc.uobaghdad.edu.iq

(Received August 17, 2024; received in revised form November 21, 2024; accepted November 30, 2024)

The dielectric barrier discharge (DBD) plasma is one of the branches of plasma produced at atmospheric pressure. It is easy to use in the laboratory, where the dielectric barrier discharge was built from a copper electrode with a glass insulator in front of one of the electrodes. The plasma was generated between the two electrodes at a high applied voltage ranging between (5-9) kV using a high voltage power supply and at a (7) kHz frequency. To perform the spectral characterization of the plasma produced by the dielectric barrier discharge (DBD) system and calculate the plasma parameters, a gradually increasing voltage (5-9) kV was used with a fixed frequency of (7) kHz in the first case, and in the other case, the frequency was changed (5-9) kHz with a constant applied voltage of (8) kV. The results showed that the increased applied voltage and frequency value led to an increase in the spectral intensity of (N_2) of the plasma generated between the two electrodes, ranging from (296.44 - 715) nm. As well as an increase in the plasma electron temperature (T_e) (0.895-1.436) eV and (0.922-0.522) eV, and the resulting plasma number density (n_e) (5.485-9.541) x10^{16} cm^{-3} and (4.856-8.090) x10^{16} cm^{-3} in both cases, respectively, as well as the rest of the other plasma parameters.

Key words: DBD system, plasma parameters, Stark broadening, electron temperature, plasma spectrum intensity.
PACS number(s): 79.60.Cn.

1. Introduction

Gas discharge plasmas, sometimes referred to as low-temperature plasmas, have garnered significant interest in recent decades due to their crucial role in numerous technological advancements. Subsequently, plasma technologies have applications in other technological and research domains, such as microelectronics, gas lasers, and polymer processing [1, 2]. Dielectric barrier discharge (DBD) is considered one of the most cost-effective producers of non-thermal plasma among various plasma sources [3, 4]. This discharge is recognized for its efficacy in beginning chemical and physical gas processes [5–7]. Consequently, the majority of plasma-generating systems are considered to be fundamental and essential systems because they are utilized in a considerable number of technological and research applications [5, 8]. Microelectronics, lasers, and related areas are included. The voltage discharge barrier is one system that can be utilized to process food, fruits, meat, vegetables, and other foods [9–11]. Plasma-generating systems are crucial in simplifying complex tasks in laboratory circumstances, such as dealing with atmospheric pressure and forming plasma between the poles. This efficiency reassures us of their potential in various applications, including cancer cell treatment, wound healing, and environmental purification [12]. To facilitate the handling of the dielectric barrier discharge, an insulator must be used between the two poles made of a specific material [13]. The air jet plasma and the dielectric barrier discharge continue to be at the top of the list of instruments that are considered to be among the most versatile, simple to run, and straightforward to deploy plasma generators [14, 15]. DBD has undergone thorough examination in recent years due to its prospective utilization in various domains [8]. It encompasses both material processing and applications in the energy and environment sectors [16]. It can generate highly reactive plasma at nearly ambient temperature, with low energy consumption, utilizing a straightforward reactor setup under atmospheric pressure settings [5,

9]. The domain of diagnostics in created plasma is extensive and varied, with diagnostic instruments serving as a crucial component for comprehending the behavior of the produced plasma [17]. Numerous diagnostic techniques are available, contingent upon the type of plasma produced and the requisite information, and are commonly utilized in academic settings; the analysis of the waveforms of the driving current and voltage is crucial for understanding the primary processes occurring during the discharge [17, 18]. The second instrument signifies an electrical probe utilized in low-pressure and low-temperature plasma environments. The third tool signifies mass spectrometry, conducted at the substrate borders, and does not significantly impact the plasma. The fourth instrument is optical emission spectroscopy, which is appropriate for application with a dielectric barrier discharge to analyze the spectral response produced during plasma generation between the two electrodes [19]. Various techniques are employed to quantify plasma characteristics, such as plasma electron temperature and electron density. However, optical emission is the most commonly utilized method [18], [19]. The optical emission spectroscopy (OES) method is frequently employed for optical characterization[20]. Most of the processes occurring in plasma are the result of collisional, radiational, excitational, and de-excitational processes that are in equilibrium with each other [14]. Therefore, at thermodynamic equilibrium (TE), all processes are balanced within the plasma, and its temperature can be determined. While at local thermal equilibrium (LTE), this means that the emission is generated somewhere in the plasma and absorbed somewhere else. Therefore, in such equilibrium, the energy loss through radiation (unabsorbed radiation) is slight compared to the energy involved in other processes (collisions), so local thermal equilibrium (LTE) can be assumed, and the plasma parameters for this case can be calculated. The LTE's electron temperature (Te eV) is calculated using the following equation [1,2].

$$ln\left[\frac{\lambda_{ji}I_{ji}}{hcA_{ji}g_j}\right] = -\frac{1}{KT}\left(E_j\right) + \ln\left|\frac{N}{U(T)}\right| \quad (1)$$

Where g denotes the statistical weight, λ denotes the wavelength, E is the excited state energy in eV, I_{ji} denotes the intensity, A_{ji} denotes the transition probability, N denotes the density of the state's population, and k denotes the Boltzmann constant [21, 22]. In plasma spectrum research, stark broadening is crucial in widening spectral lines [23]. It provides information on the electron density at a specific plasma electron temperature [24, 25]. The electron density can be determined by applying the following equation.

$$n_e = \left[\frac{\Delta\lambda}{2\omega_s}\right] N_r \ (cm^{-3}) \quad (2)$$

Where Δλ the full width at half maximum (FWHM) nm of the line ωs is the Stark broadening parameter in the standard tables, and N_r is the reference electron density [21, 23]. The frequency of plasma is calculated using the following equation.

$$f_p = 8.98\sqrt{n_e}\ (\text{Hz}) \quad (3)$$

Plasma frequency is a fundamental property exclusively determined by density [26]. Plasma exhibits a high frequency due to the minuscule mass of electrons [27]. Debye shielding, also known as Debye length (λ_D), is a phenomenon in which charged particles in a plasma respond to an electric field in a way that diminishes its effect on the local fields [28, 29]. This results in the plasma exhibiting quasi-neutrality. The Debye length (λ_D) is defined as [21].

$$\lambda_D = \sqrt{\frac{\varepsilon_o K_B T_e}{n_e e^2}} = 743 \times \sqrt{\frac{T_e}{n_e}} \quad (cm) \ (4)$$

Hence, this study aims to diagnose and quantify the plasma parameters of the dielectric barrier discharge (DBD) system and illustrate the impact of gradually increasing the applied voltage and frequency on the plasma's properties.

2. Experimental part

Figure 1 shows a schematic of the dielectric barrier discharge (DBD) system manufactured in the laboratory, where copper was used to manufacture the dielectric barrier discharge electrodes and was insulated by a thermal insulator with the two electrodes of the system arranged vertically. The total diameter of the copper electrode is (5 mm), and the outer diameter of the thermal insulator inside which the copper electrode is placed is 60 mm. A high voltage (AC) power supply was used with a peak of 25 kV and worked on an increasing voltage starting from (5-9) kV with a fixed frequency at 7 kHz, and a

rising frequency was also used from (5-9) kHz with a fixed applied voltage at 8 kV to study the effect of increasing the applied voltage and increasing the frequency on the properties and parameters of the plasma. The upper cathode electrode of the dielectric barrier discharge was connected to the high voltage device as well as the anode electrode, and the distance between the two electrodes was 5 mm, with the use of a piece of glass with a thickness of 2 mm that was placed between the two electrodes during plasma generation. To diagnose the plasma and collect the resulting spectrum, a laboratory spectrometer (S3000-UV-NIR) operates between (250-1100) nm, with the optical fiber fixed by a metal holder and 1 cm away from the plasma-generating electrodes. These recorded data were analyzed and matched with the National Institute of Technology and Standards (NIST) data [30].

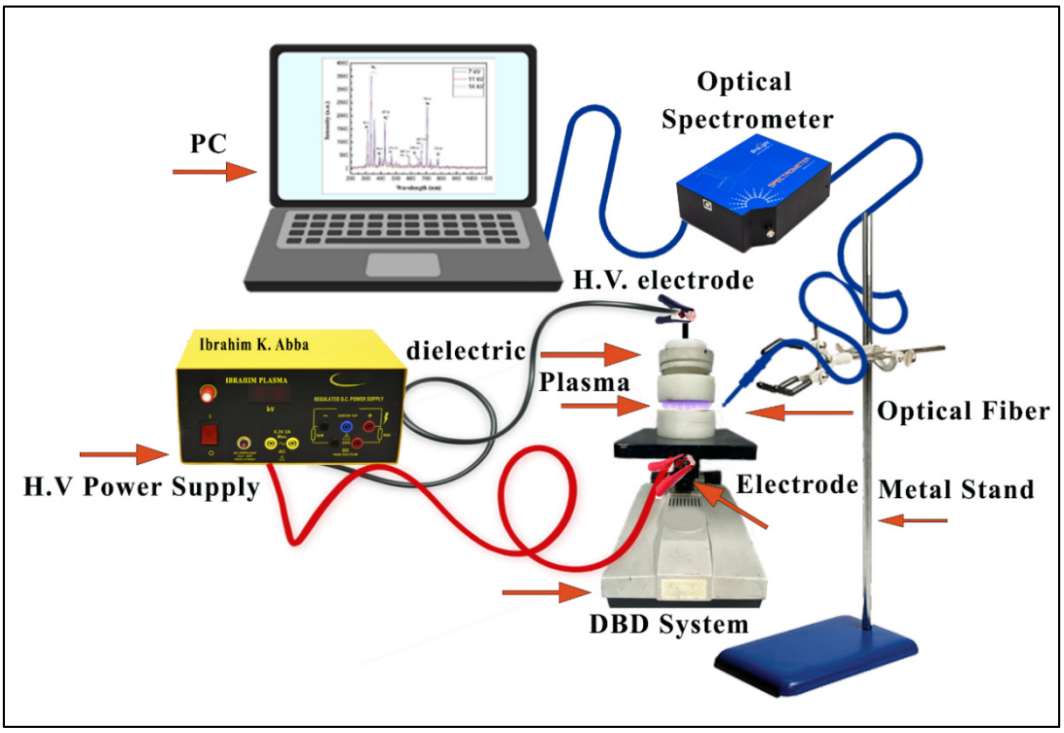

Figure 1 – Schematic diagram of the dielectric barrier discharge (DBD) system and setup of the optical spectrometer

3. Results and discussions

Analyzing the plasma spectrum produced by the dielectric barrier discharge is crucial for determining the remaining plasma parameters, making emission spectral diagnosis a highly significant technique. Under normal atmospheric pressure, an extensive and multi-peaked spectrum of nitrogen gas was acquired. The emission spectrum depicted in Fig. 2 exhibits many peaks spanning from 280 to 750 nm. These peaks were detected by the spectral diagnostic tool at a frequency of 7 kHz, while the applied voltage ranged from (5-9) kV, and the distance between the upper and lower electrodes was 5 mm. The emission spectrum analysis revealed many peaks corresponding to molecular nitrogen [31]. These peaks were observed at wavelengths ranging from 296.44 nm to 419.53 nm, with a prominent nitrogen peak at 336.38 nm. Additionally, nitrogen ionic peaks were detected at 672.94 nm and 715 nm. The spectral results indicate that increasing the applied voltage from 5 to 9 kV results in a proportional increase in the emitted intensity of the plasma spectrum. This increase in intensity is attributed to the higher energy supplied to the electrons, leading to a more significant number of collisions and the excitation of multiple molecules during the emission process [23].

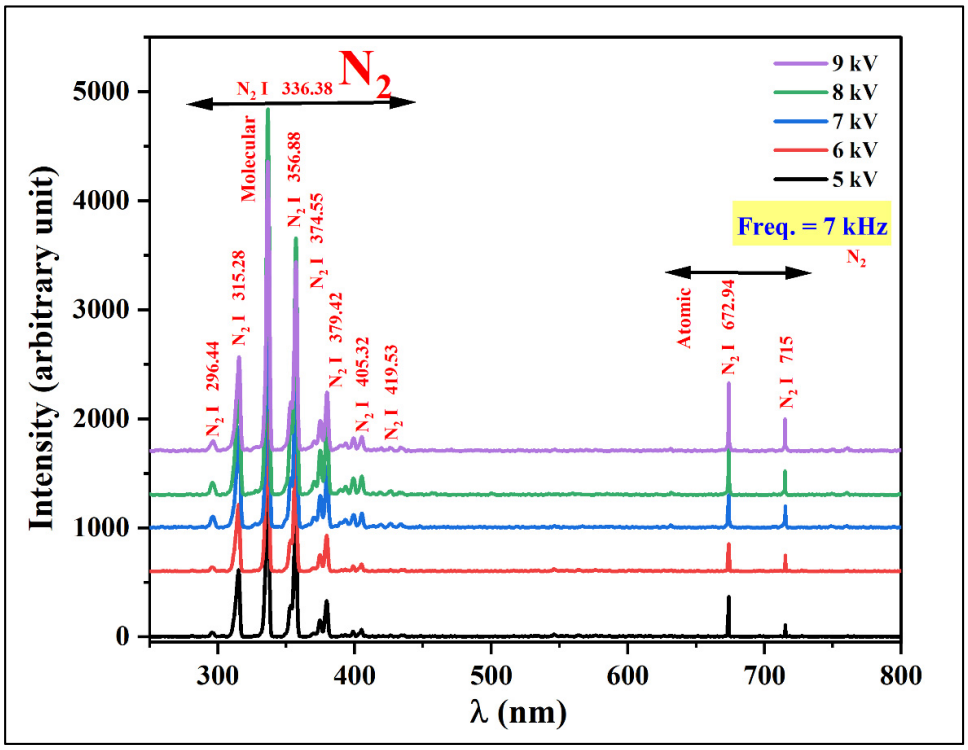

Figure 2 – The plasma spectrum from a dielectric barrier discharge at an increased applied voltage (5-9) kV and a fixed frequency of 7 kHz

Figure 3 displays the plasma spectrum produced by the dielectric barrier discharge under a fixed applied voltage of 8 kV. As the frequency value gradually increases from 5 to 9 kHz, the intensity of the emitted spectrum also increases. Additionally, the spectrum reveals the presence of multiple nitrogen peaks (N_2I) at specific wavelengths, namely 295.88, 314.64, 336.60, 374.55, 379.15, 398.87, 405.05, and 419.27 nm. The highest intensity of spectral emission occurs at 335.83 nm. When comparing the emitted spectra under increased applied voltage and frequency, we observe a consistent increase in the spectral emission intensity. Notably, the intensity is slightly higher when the frequency is increased. This can be attributed to the heightened collisions between molecules within the confined space between the electrodes, and these findings align closely with [20, 22].

To determine the plasma parameters and understand how they change in the dielectric barrier discharge (DBD) system with increasing applied voltage and frequency, the Boltzmann plots equations were employed to calculate the electron temperature (T_e), as shown in Eq. 1. The results demonstrated a progressive rise in the plasma electron temperature as the applied voltage increased, indicating a strong correlation between the two variables. The slope of the fitted line is represented by the fraction ($-1/T_e$), where (T_e) is a specific value. R^2 is a mathematical coefficient that quantifies the quality of a linear fit, with values ranging from 0 to 1. For each equation that fits inside the spectral range of the fitting line, as depicted in Fig. 4.

The findings demonstrated a progressive rise in the electron temperature values, ranging from 0.895 to 1.436 eV, as the applied voltage gradually increased. Similarly, the electron temperature was determined using Boltzmann plots equations when the frequency values rose within the range of (5-9) kHz, as shown in Fig. 5. The electron temperature varied within the range of (0.922 - 1.522) eV as the frequency increased gradually, with a modest rise observed in the first situation of applied voltage[32]. The electron temperature values in two cases increase due to the doubling of the discharge between the upper and lower electrodes, resulting from the increased energy supplied by the high voltage supply. This increase in energy leads to an increase in the discharge voltage; these findings are in agreement with the researchers' findings and are relatively near to them [31, 33].

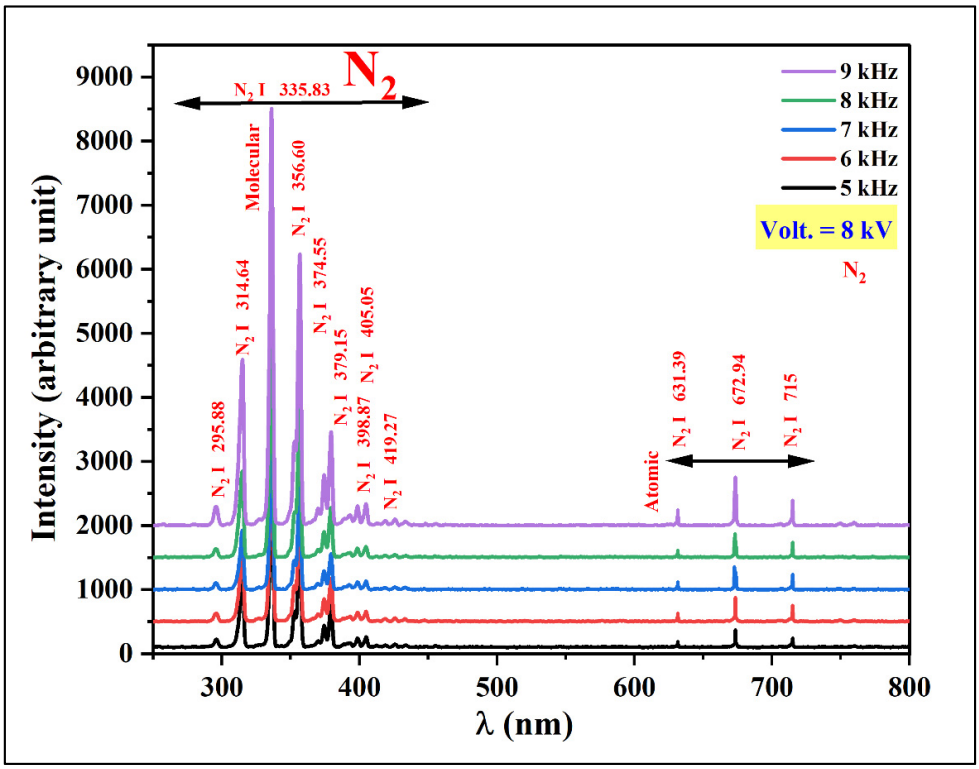

Figure 3 – The plasma spectrum from a dielectric barrier discharge at an increased frequency (5-9) kHz and a fixed applied voltage of 8 kV

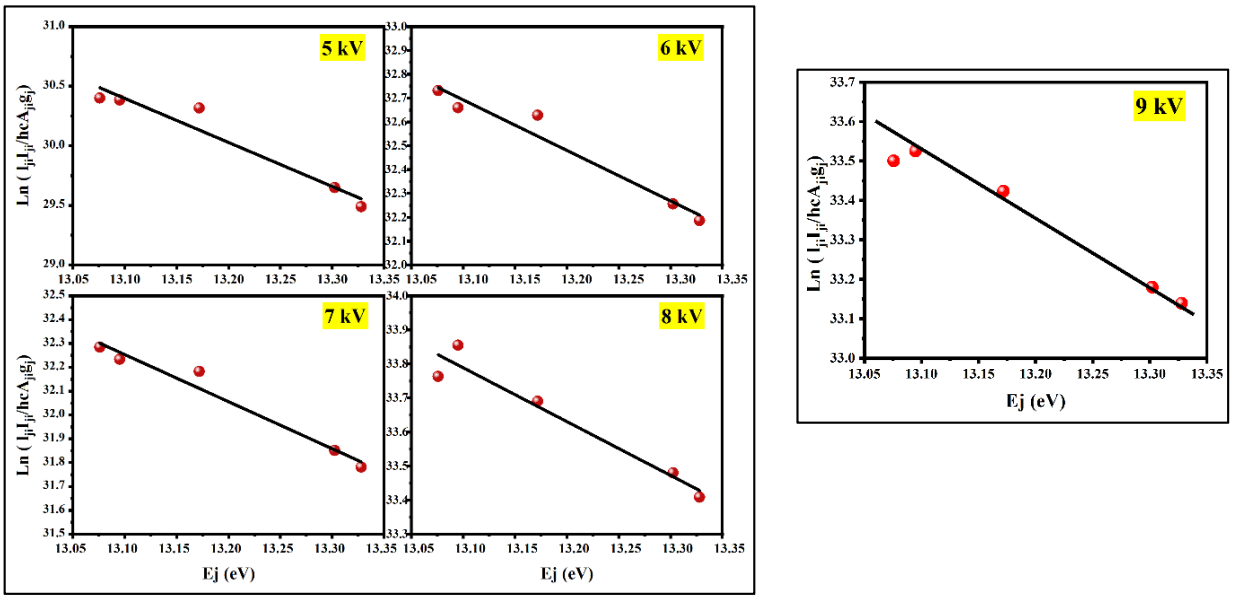

Figure 4 – Boltzmann plots at different applied voltage (5-9) kV to calculate the electron plasma temperature in dielectric barrier discharge (DBD)

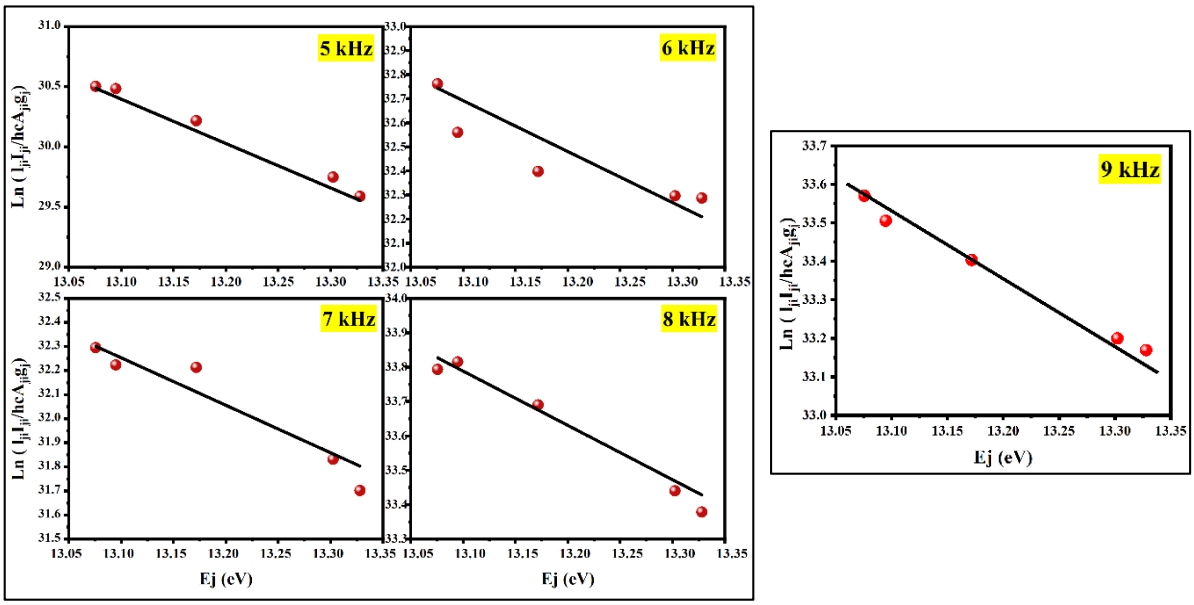

Figure 5 – Boltzmann plots at different frequencies (5-9) kHz to calculate the electron plasma temperature in dielectric barrier discharge (DBD)

We utilized Lorentzian fitting to calculate the full width at the mid-peak to determine the plasma electron density as in Eq. 2. This calculation was performed when the applied voltage and frequency were increased. The Stark effect was employed, considering the broadening values for 356.88 nm and 335.83 nm wavelengths, respectively. Tables 1 and 2 show the experimental data results for the full-width half-maximum parameters (FWHM) for the 356.88 and 335.83 nm wavelengths, where Fig. 6 also shows the gradual increase in wave intensity for each value of the applied voltage or frequency. Measuring the full-width half-maximum parameter (FWHM) is necessary to calculate the electron density in the resulting plasma in both cases. Fitting the observed profiles provides a very accurate total density, including spectral line broadening. It is noticeable that the electron density value increases (5.485-9.541) x 10^{16} (cm^{-3}) significantly when the full-width half maximum increases from (0.232-0.414) nm when the applied voltage increases, and in the same way when the frequency increases, the electron density value increases (4.856-8.090) x 10^{16} (cm^{-3}) at full-width half maximum range (0.211-0.344) nm, these results of electron density are aligned and coherent with the researchers' findings [20, 22]. Figure 6 illustrates these results, which indicate that both the applied voltage and frequency increase led to an expansion of the mid-peak width.

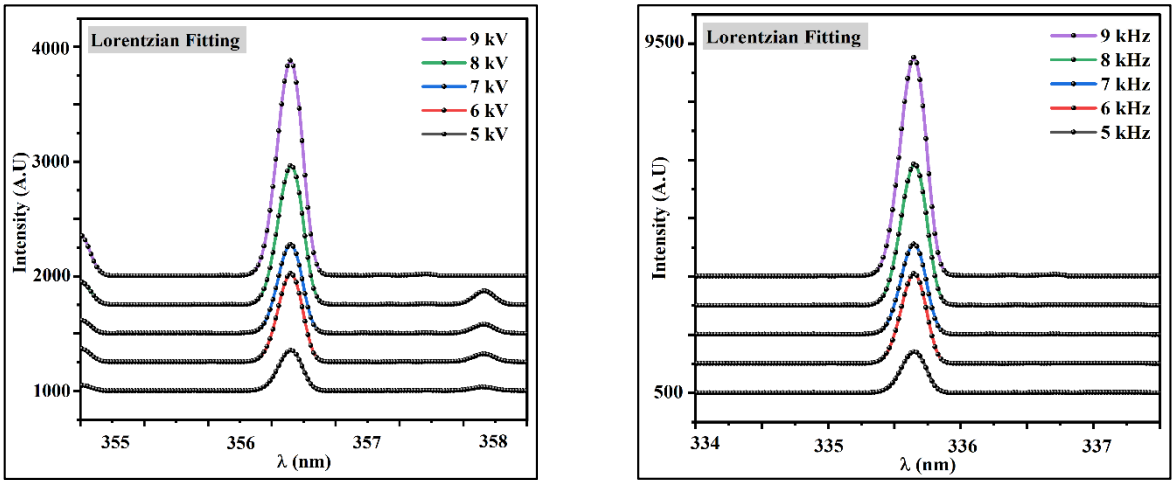

Figure 6 – Lorentzian fitting of line broadening for different applied voltage (5-9) kV and frequency (5-9) kHz

Figures 7 and 8 depict the variation in electron temperature and density as the applied voltage gradually increases while keeping the frequency fixed at 7 kHz. Additionally, they illustrate the increase in frequency ranging from 5 to 9 kHz while maintaining a fixed voltage of 8 kV in the dielectric barrier discharge (DBD) system. The two figures indicate that the plasma electron temperature (T_e) and electron density (n_e) progressively rise with increasing supplied voltage or frequency. This suggests an enhancement in the electric field intensity within the generated plasma, as the electric field increasingly accelerates free electrons, resulting in more frequent collisions with neutral gas atoms and molecules possessing higher energy. These collisions can ionize neutral particles, generating more free electrons and ions and resulting in a substantial rise in plasma electron temperature and electron density. This also applies when the frequency is incrementally raised while maintaining a constant applied voltage value. Augmenting the frequency will result in elevated collision rates since electrons acquire more incredible energy from the electric field prior to colliding with neutral particles, hence increasing their thermal energy due to the heightened frequency. Consequently, the plasma electron temperature and electron density will rise [20, 26].

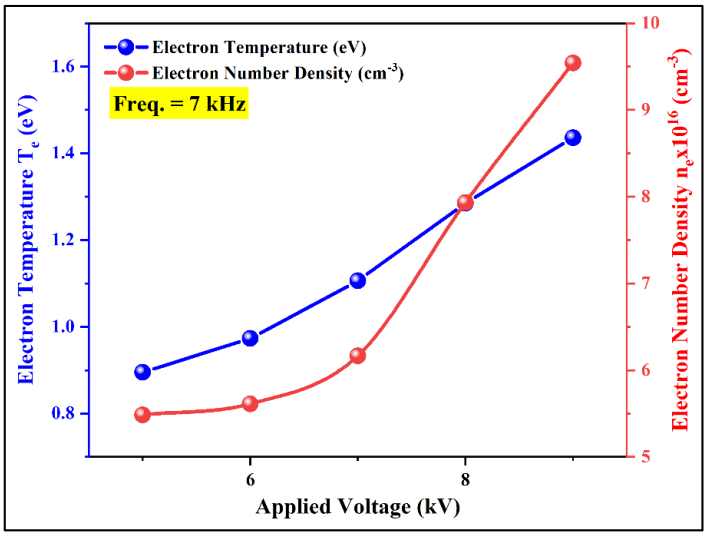

Figure 7 – The electron temperature (Te) and electron density (ne) versus the increased applied voltage (5-9) kV at a constant frequency of 7 kHz

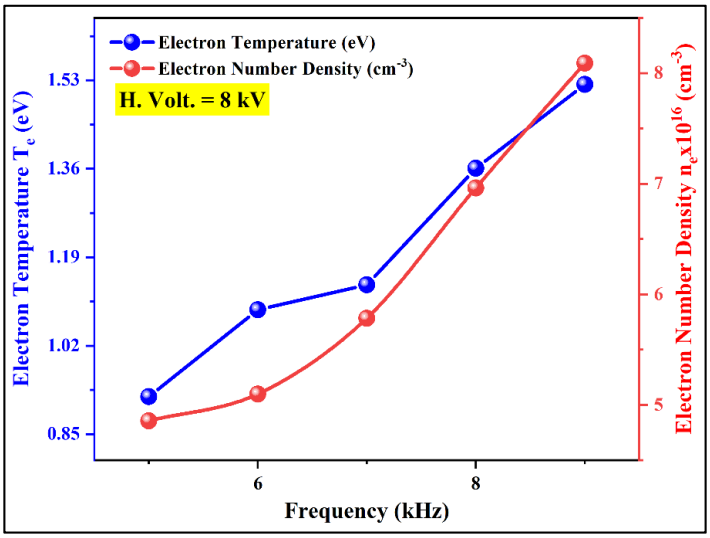

Figure 8 – The electron temperature (Te) and electron density (ne) versus the increased frequency (5-9) kHz at a constant applied voltage of 8 kV

Tables 1 and 2 display the plasma properties obtained from the earlier equations (see Eq. 3 & 4) for both increasing applied voltage and frequency cases. The tables illustrate the direct correlation between the increased applied voltage and frequency, resulting in both scenarios' consistent rise in plasma frequency (fp) values. In contrast, there is a gradual drop in the Debye barrier (λ_D) values as the frequency increases.

Table 1 – DBD Plasma Parameter in case of Increasing Applied Voltage (5-9) kV

Applied Voltage (kV)	Te (ev)	FWHM (nm)	ne x 10^{16} (cm^{-3})	fp x 10^{12} (Hz)	λ_D x 10^{-6} (cm)
5	0.895	0.232	5.485	2.082	3.001
6	0.973	0.240	5.612	2.106	3.093
7	1.106	0.267	6.165	2.207	3.147
8	1.285	0.320	7.932	2.503	2.990
9	1.436	0.414	9.541	2.745	2.883

Table 2 – DBD Plasma Parameter in case of Increasing Frequency (5-9) kHz

Frequency (kHz)	Te (ev)	FWHM (nm)	ne x 10^{16} (cm^{-3})	fp x 10^{12} (Hz)	λ_D x 10^{-6} (cm)
5	0.922	0.211	4.856	1.983	3.237
6	1.089	0.226	5.098	2.032	3.434
7	1.137	0.252	5.783	2.164	3.294
8	1.361	0.290	6.962	2.374	3.285
9	1.522	0.344	8.090	2.559	3.223

An insulator is crucial to ensure the safety of the discharge between the electrodes. When ionization occurs between the two electrodes, charges build up on the insulator. The separation between the electrodes is a crucial factor significantly influencing the plasma parameters and its diagnosis[34, 35]. It directly impacts the characteristics of the plasma generated by the dielectric barrier discharge, such as the electron temperature (T_e), electron density (n_e), electron frequency (f_p), (λ_D), and the active species formed during the discharge between the electrodes. The results acquired for the plasma parameters assessed in the dielectric barrier discharge plasma system indicate their potential applicability across diverse fields, including medical, technological, industrial, and agricultural sectors, through the plasma electron temperature, electron density, Debye length, and plasma frequency, in conjunction with the other parameters measured from the system's plasma.

4. Conclusion

This study found a strong association between the applied voltage and frequency during the discharge process between the electrodes and the resulting plasma spectrum and plasma characteristics. The elevated voltage is crucial in influencing plasma electron temperature (T_e) and electron density (n_e) values in both scenarios. Specifically, the plasma electron temperature reached a maximum value of 1.436 eV, while the electron density reached $9.541x10^{16}$ cm^{-3} at 9 kV. At the lowest voltage of 5 kV, the electron temperature (T_e) was 0.895 eV, and the electron density (n_e) was 5.485 $x10^{16}$ cm^{-3}. Similarly, increasing the frequency (5-9) kHz had a uniform effect on all plasma parameters, which closely resembled the effect of increasing the voltage. The findings also indicated that the spectrum emission strength rises proportionally with higher voltage and frequency. Additionally, many peaks were seen for nitrogen (N_2), encompassing both molecular and ionic forms. The spacing between the electrodes (5 mm) is a crucial factor in determining the production of the discharge and its uniform distribution throughout the electrode surface during the plasma generation process. Consequently, all plasma properties will be influenced.

Acknowledgement

I want to thank the Plasma Laboratory at the University of Baghdad's Department of Physics and College of Science for motivating me to pursue a scientific career after completing my academic work.

References

1. Smirnov B. M. Theory of gas discharge plasma. Springer Cham. 2015. Vol. 84. 423 p. https://doi.org/10.1007/978-3-319-11065-3
2. Braithwaite N. S. J. Introduction to gas discharges // Plasma sources Sci. Technol. - 2000. - Vol. 9. - № 4. - P. 517. https://doi.org/10.1088/0963-0252/9/4/307
3. Wong C. S., Mongkolnavin R. Elements of Plasma Technology. Springer Singapore. 2016. 123 p. https://doi.org/10.1007/978-981-10-0117-8
4. Javanmard S., Pouryoussefi S. G. Comparison of characteristics of atmospheric pressure plasma jets using argon and helium working gases // Curr. Appl. Phys. - 2023 - Vol. 46. - P. 61–69. https://doi.org/10.1016/j.cap.2022.12.002
5. Kratzer J., Burhenn S. Chapter 12 - Dielectric barrier discharge devices A. D'Ulivo and R.E.B.T.-V.G.T. for T.E.A. Sturgeon // Eds. Elsevier - 2022. P. 403–442. https://doi.org/10.1016/B978-0-323-85834-2.00006-9
6. S. Dang Li X., Yu X., Abbas G., Zhang Q., Cao L. The application of dielectric barrier discharge non-thermal plasma in VOCs abatement: A review // Chem. Eng. J. - 2020. - Vol. 388. - P. 124275. https://doi.org/10.1016/j.cej.2020.124275.
7. Abbas I. K., Adim K. A. Synthesis and characterization of magnesium oxide nanoparticles by atmospheric non-thermal plasma jet, Kuwait // J. Sci. - 2023. - vol. 50. - № 3. - P. 223–230. https://doi.org/10.1016/j.kjs.2023.05.008
8. Haji A., Barani H. Chapter 1 - Introduction of plasma technology in The Textile Institute Book Series // S. Ul Islam and A. B. T.-A. in P. T. of T. S. Haji, Eds. Woodhead Publishing. 2024. - P. 1–12. https://doi.org/10.1016/B978-0-443-19079-7.00002-6
9. Laroussi M. The dielectric barrier discharge and the start of a beautiful friendship: Personal remembrance of Dr. Ulrich Kogelschatz // Plasma Chem. Plasma Process. - 2023. - Vol. 43. - №. 6. - P. 1287–1292. https://doi.org/10.1007/s11090-023-10313-2
10. Conrads R. A., Schmidt M. Plasma generation and plasma sources // Plasma Sources Sci. Technol. - 2000. - Vol. 9. - .№ 4. P. 441–454. https://doi.org/10.1088/0963-0252/9/4/301.
11. Kasa U., Juswono P., Santjojo D. J. D. H. Identification of reactive species produced by surfaces dielectric barrier discharge nonthermal plasma with gas sources variation (Air, N2, O2) to kill bacteria // J. Penelit. Pendidik. IPA - 2022. - vol. 8. - №. 4. P. 2371–2377. https://doi.org/ 10.29303/jppipa.v8i4.2167.
12. Kadhim A. A., Abbas B. K. Preparation of cobalt oxide nanoparticles by atmospheric plasma jet and investigation of their structural characteristics // Egypt. J. Chem. - 2022. https://doi.org/10.21608/ejchem.2022.146951.6414.
13. Rodrigues F., Pascoa J., Trancossi M. Heat generation mechanisms of DBD plasma actuators // Exp. Therm. Fluid Sci. - 2018. - Vol. 90. - P.55–65. https://doi.org/10.1016/j.expthermflusci.2017.09.005
14. Goldston R. J. Introduction to plasma physics // CRC Press - 2020. https://doi.org/10.1201/9780367806958.
15. Aadim K. A., Abbas I. K. Synthesis and Investigation of the structural characteristics of zinc nanoparticles produced by an atmospheric plasma // Jet. -2023. - Vol. 64. - №. 16. P. 10. https://doi.org/10.24996/ijs.2023.64.4.15.
16. Nguyen T. M., Kaushik N., Nguyen T. T., Choi E. H., Nguyen L. N., Kaushik N. K. The outlook of flexible DBD-plasma devices: Applications in food science and wound care solutions // Mater. Today Electron. - 2024. - Vol. 7. - P. 100087. https://doi.org/10.1016/j.mtelec.2023.100087.
17. Huo J. et al., Effects of chemically reactive species generated in plasma treatment on the physico-chemical properties and biological activities of polysaccharides: An overview // Carbohydr. Polym. - 2024. - Vol. 342 - P. 122361. https://doi.org/10.1016/j.carbpol.2024.122361.
18. Zaplotnik R., Primc G., Vesel A. Optical emission spectroscopy as a diagnostic tool for characterization of atmospheric plasma jets // Appl. Sci. - 2021. - Vol. 11. - №. 5. - P. 1–22. https://doi.org/10.3390/app11052275.
19. Asenjo-Castillo J., Vargas-Blanco I. Espectroscopia de Plasmas en condiciones de presión atmosférica // Rev. Tecnol. en Marcha - 2016. - Vol. 29. - № 6. - P. 47. https://doi.org/10.18845/tm.v29i6.2901.
20. Liu P., He L., Zhao B. Discharge and optical emission spectrum characteristics of a coaxial dielectric barrier discharge plasma-assisted combustion actuator // J. Spectrosc. - 2020. - Vol. 2020. - P. 6034848. https://doi.org/10.1155/2020/6034848.
21. Abbas I. K., Aadim K. A. Spectroscopic diagnosis of cobalt plasma produced by OES technique and influence of applied voltage on plasma parameters // Iraqi J. Sci. - Vol. 64. - №. 5. - P. 2271–2281. https://doi.org/10.24996/ijs.2023.64.5.15.
22. Kadhim M. M., Abbas Q. A., Abdulameer M. R. Study of some plasma characteristics in dielectric barrier discharge (DBD) system // Iraqi J. Sci. - 2022. - Vol. 63. - № 5. - P. 2048–2056. https://doi.org/ 10.24996/ijs.2022.63.5.20
23. Rosato J. Effect of collisions on motional Stark broadening of spectral lines // J. Quant. Spectrosc. Radiat. Transf. - 2023. - Vol. 306. - P. 108628. https://doi.org/10.1016/j.jqsrt.2023.108628.
24. Tapalaga I., Traparić I., Trklja N. Boca, J. Purić, Dojčinović I. P. Stark spectral line broadening modeling by machine learning algorithms // Neural Comput. Appl. - 2022. - Vol. 34. . №8. P. 6349–6358. https://doi.org/ 10.1007/s00521-021-06763-4.
25. Zenkhri D. E., Meftah M. T., Khelfaoui F. Screening and relativistic effects on the stark broadening of hydrogenic ion lines in a plasma // High Energy Density Phys - 2023. - Vol. 46. - P. 101035. https://doi.org/10.1016/j.hedp.2023.101035
26. Shrestha R., Subedi D. P., Gurung J. P., Wong C. S. Generation, characterization and application of atmospheric pressure plasma jet // Sains Malaysiana - 2016. - Vol. 45. - №. 11. - P. 1689–1696.
27. Shahrbabaki A. N., Bazazzadeh M., Khoshkhoo R. Investigation on supersonic flow control using nanosecond dielectric barrier discharge plasma actuators // Int. J. Aerosp. Eng - 2021. - Vol. 2021. - P. 2047162. https://doi.org/ 10.1155/2021/2047162
28. Lee S., Lim H. Debye shielding of an electron in various plasma distributions // J. Korean Phys. Soc -2022. - Vol. 80. - №. 2. - P. 153–160. https://doi.org/10.1007/s40042-021-00336-3
29. Orabi T. F., Aadim K. A. Spectroscopic diagnosis of nickel and zinc plasmas produced by plasma jet technique // J. Opt - 2024. https://doi.org/ 10.1007/s12596-024-01891-1.
30. Kramida A., Fuhr J.R. NIST DataBase // Physical Measurement Laboratory - 2023, https://doi.org/10.18434/T46C7N.

31. Khaleel S. F.,. Abbas Q. A. Influence of dielectric media on the plasma characteristics in DBD Discharge // Iraqi J. Sci.,-2022. -P. 2470–2481. https://doi.org/ 10.24996/ijs.2022.63.6.13.

32. Park S., Choe W., Moon S. Y. Yoo S. J. Electron characterization in weakly ionized collisional plasmas: from principles to techniques // Adv. Phys. X. - 2019. - Vol. 4. - № 1. https://doi.org/ 10.1080/23746149.2018.1526114.

33. Dilecce G., Ambrico P. F., Martini L. M., Tosi P. On the determination of the vibrational temperature by optical emission spectroscopy // Plasma Sources Sci. Technol. - 2022. - Vol. 31. - №. 7. - P. 77001. https://doi.org/ 10.1088/1361-6595/ac7f54.

34. Fikry M., Tawfik W., Omar M. Measurement of the electron temperature in a metallic copper using ultrafast laser-induced breakdown spectroscopy // J. Russ. Laser Res - 2020. - Vol. 41. - №. 5. P. 484–490. https://doi.org/ 10.1007/s10946-020-09901-w.

35. Jakob H., Kim M. K. Generation of non-thermal plasmas over large and complex surfaces // Plasma Res. Express. - 2020. - Vol. 2. - №. 3. https://doi.org/ 10.1088/2516-1067/abb2fd.

Information about authors:

Abbas Ibrakhim Karim, associate professor at the University of Baghdad-College of Science-Dept. of Physics (Iraq) e-mail: Ibrahim.kareem1104a@sc.uobaghdad.edu.iq